Received: 5 October 2020 | Revised: 11 December 2020 | Accepted: 12 December 2020

DOI: 10.1002/pat.5198

RESEARCH ARTICLE

polymers for advanced technologies WILEY

Synergistic contribution on flame retardancy by charring production in high-performance PEI/PBT/PTFE ternary blends: The role of PTFE

Mauricio Vásquez-Rendón[1] | Manuel Romero-Sáez[1] | Jhorman Mena[1] | Victor Fuenzalida[2] | Isadora Berlanga[3] | Mónica L. Álvarez-Láinez[4]

[1]Grupo Calidad, Metrología y Producción, Instituto Tecnológico Metropolitano, Medellín, Colombia

[2]Departamento de Física, Facultad de Ciencias Físicas y Matemáticas, Universidad de Chile, Santiago, Chile

[3]Departamento de Ingeniería Química, Biotecnología y Materiales, Facultad de Ciencias Físicas y Matemáticas, Universidad de Chile, Santiago, Chile

[4]Grupo de Investigación en Ingeniería de Diseño, Universidad EAFIT, Medellín, Colombia

Correspondence
Mauricio Vásquez-Rendón, Grupo Calidad, Metrología y Producción, Instituto Tecnológico Metropolitano, Campus Robledo, Calle 73 No. 76A - 354, Medellín, Colombia.
Email: mauriciovasquez@itm.edu.co

Funding information
Fondecyt, Grant/Award Number: 11190841; Program VID in the framework of "U-Inicia", Grant/Award Number: UI 003/2018

High-performance binary blends between poly(ether imide) (PEI) and flame-retardant poly(butylene terephthalate) (PBT) are modified with 5, 10, and 15 wt% of poly(tetrafluoroethylene) (PTFE) using a two-step melt-processing method. Morphology study reveals that PTFE does not interfere with PEI and PBT interfacial interaction during blends fabrication, and the dual-phase inversion observed for binary PEI/PBT blends in previous works remains the same. Thermal degradation and fire resistance analyses show that charring layer formation is the major flame protection process and that PTFE enhances charring production for ternary blends. According to UL94 horizontal burning test, all blends are categorized as slow-burning materials. Bomb calorimetry and thermal gravimetric analyses reveal that there is an interaction between PTFE with PEI and PBT phases, as well as with their degradation products. This phenomenon is explained by X-ray photoelectron spectroscopy analysis, and it is attributable to Sb-F species which enhances the formation of an intumescent layer.

KEYWORDS
charring formation, flammability, PEI/PBT/PTFE, Sb-F species, thermal degradation

1 | INTRODUCTION

The increasingly demanding applications in the modern world lead users to wear extra protection in their garments, uniforms, architectonic structures, or protective housing of electronic devices, to face the hazardous conditions to which they are exposed.[1-4] Along these lines, industries such as electronics, automotive, nautical, and aerospace have forced the materials safety standards to be higher and stricter,[5-7] and one of the materials property that has gained great importance is flame retardancy. Polymeric materials are the most widely used in these industries worldwide, due to their good performance/price and performance/weight ratios. Some of these polymers are flame-retardants by themselves, while others must be filled or mixed with inorganic materials to achieve such properties.[8-10]

In recent decades, flame retardancy properties of several polymers have been studied, and new developments to improve their flame performance are proposed.[8] Some of the most important is the incorporation of clays to the polymer matrix, such as melamine triazine and bentonite to *different polymeric matrices*,[11-13] and biobased additives addition, such as tannic acid or polydopamine,[14,15] which counteract the toxicity of common halogenated additives. Nevertheless, some of these developments lead to decreasing the processability and mechanical properties of polymers due to the high concentrations of fillers required to reach fire retardancy properties (>40 wt%).[16]

Other strategy that could be used to improve flame retardancy is based on polymer blend formulations.[17-23] Polymer blending is a versatile way of obtaining new materials by combining existing ones, where the advantage of one component should compensate for the deficiencies of the other.[24] For instance, materials with high thermal stability and inherent charring formation, which is the most effective protection against flame propagation, could be blended with low

viscosity materials.[2,25-30] This will result in new materials with remarkable thermal and flame retardancy properties, together with excellent processability.

In this work, we use blending technology to modify the thermal and flame resistance properties of binary PEI/PBT blends by means of a melt-processing method. The third component must provide high thermal stability, flame resistance, and do not affect blends processability. For this purpose, we use 5, 10, and 15 wt% of poly(tetrafluoroethylene) (PTFE), which is a high-performance polymer commonly used as a filler in the solid-state to form polymer composites, or as a new phase to produce polymer blends from solution or melt blending.[31-39] We evaluate the role of PTFE on the processability, morphology, thermal stability, and flame resistance of PEI/PBT/PTFE blends. It is found that PTFE does not have a negative effect on blends processability, and that the same phase inversion phenomenon observed in binary PEI/PBT blends was revealed for ternary blends. Additionally, an explanation for flame protection improvement that occurs during burning tests and thermal analysis, is proposed based on the characterization of blends before and after flammability tests using scanning electron microscopy (SEM), thermogravimetric analysis (TGA), and X-ray photoelectron spectroscopy (XPS).

2 | MATERIALS AND METHODS

2.1 | Materials and blends fabrication

Ternary PEI/PBT/PTFE blends were fabricated by mixing commercial grade poly(ether imide) (PEI) Ultem 1000, poly(butylene terephthalate) (PBT) Valox 301SE0 [filled with antimony trioxide crystals (Sb_2O_3) and bromide compounds], and micronized powder of PTFE Lanco 1972. Materials were vacuum dried at 110°C for 16 hours and mixed under a standard atmosphere in a Haake Rheomix 3000 OS internal mixer fitted with roller type rotors. A two-step melt-processing method developed in our previous works to obtain binary PEI/PBT blends was used, and the main processing parameters such as processing temperature (Tp), rotors speed (n), and mixing time (t) were kept the same.[30,40] In this work, PTFE powders and PEI pellets were manually pre-mixed and homogenized together in the mixer, before the PBT phase was added. Concentrations of 5, 10, and 15 wt% PTFE were added to 50/50, 60/40, 70/30, and 80/20 PEI/PBT combinations. The amount of each phase was calculated using Equation (1):

$$m = \rho_B V f, \tag{1}$$

where ρ_B is the density of the blend calculated from polymer densities (ρ_{PEI} = 1.27 g/cm^3; ρ_{PBT} = 1.4 g/cm^3; ρ_{PTFE} = 2.2 g/cm^3) and their weight fraction in each blend formulation, V is the free volume inside the mixing chamber (V = 310 cm^3 for roller type rotors), and f is the filling factor (f = 0.9).

Table 1 lists the weight percentage and amount of each polymer, as well as the nomenclature of each produced ternary blend.

2.2 | Phases distribution

Qualitative evaluation of the homogenization degree and the presence of all components in blends was studied using a SEM JOEL JSM-7100. The samples were immersed in liquid nitrogen for 20 minutes, mechanically cryofractured, and later coated with a gold layer.

2.3 | Flammability test and thermal characterization

Flammability of blends was studied according to UL 94 standard for "Plastic Materials for Parts in Devices and Appliances." Horizontal burning (HB) tests were performed on specimens of 125 mm length, 10 mm width, and 3 mm thickness obtained in a HAAKE MiniJet Pro Injection System from Thermo Scientific. All tests were made by

TABLE 1 Composition and designation of ternary PEI/PBT/PTFE blends with 5, 10, and 15 wt% PTFE

PEI/PBT proportion	PEI (wt%)	PBT (wt%)	PTFE (wt%)	PEI/PBT/PTFE blends designation
50/50	48	47	5	48/47/5
	45	45	10	45/45/10
	43	42	15	43/42/15
60/40	57	38	5	57/38/5
	54	36	10	54/36/10
	51	34	15	51/34/15
70/30	67	28	5	67/28/5
	63	27	10	63/27/10
	60	25	15	60/25/15
80/20	76	19	5	76/19/5
	72	18	10	72/18/10
	68	17	15	68/17/15

triplicate and photographically and video recorded to calculate the average flammability rating.

The heat released from combusting blends was measured in a bomb calorimeter Parr Instrument model 1341 and an oxygen bomb Parr 1108 was used. The higher heating values (HHV) were obtained according to Parr company instructions sheets 205M and 204M to 1.0 g samples. The water temperature change was measured with a thermometer with a resolution of 0.01°C.

Thermal stability of blends was studied by means of TGA using a TGA Q500 model from TA Instruments. Samples of 40 ± 2 mg were heated within a temperature range of 25°C to 900°C at a heating rate of 10°C/min, under nitrogen atmosphere.

2.4 | XPS characterization

XPS measurements were carried out at room temperature using a Physical Electronics 1257 system with a hemispherical analyzer and nonmonochromatic radiation (Al-Kα, 1486.6 eV), operating at 200 W with working pressures in the range of 10^{-5}–10^{-6} Pa and using narrow scans (pass energy 44.75 eV and step size 200 meV). The spectra were calibrated to the C 1s core level binding energy at 285.0 eV. To detect all the elements at the surface, a survey scan of each sample was recorded before acquiring the narrow scans. The XPS spectra were adjusted using the CASA XPS software with a Gaussian-Lorentzian mix function and Shirley or Linear background subtraction. The examined residual plots for each element indicated just noise with percentages values less than 2%.

3 | RESULTS AND DISCUSSION

3.1 | Blends processing

Ternary PEI/PBT/PTFE blends are fabricated using the same processing parameters of binary PEI/PBT blends described in previous works, where PEI is homogenized at 330°C for 10 minutes, followed by PBT addition at 280°C and mixing for 3 minutes.[30,40] Neither of these temperatures or mixing times leads to PTFE thermal decomposition since thermal analyses show it melts at 320°C and its degradation temperature appears at 485.4°C, as presented in Figure S1.

Figure 1 shows the torque and temperature evolution as a function of time for a 67/28/5 blend (left), and the comparison with a binary PEI/PBT blend with equivalent PEI and PBT concentrations (right). Unlike binary blends, ternary blends are processed by feeding PTFE together with PEI during step 1 to enhance PEI and PTFE phases homogenization. It is noticed that only 5 wt% of PTFE reduces the initial torque by 75% due to the low coefficient of friction of PTFE in its solid-state.[41,42] When it stabilizes and reaches 79 Nm, PEI and PTFE are properly integrated and PBT can be added in step 2. After 13 minutes, all phases are homogenized and the torque stabilizes at 47 Nm. At the end of steps 1 and 2, ternary blends exhibit higher torques than those of binary blends, by 58% and 88%, respectively. This is explained by the high viscosity of PTFE in its solid-to-melt transition. Some authors report that PTFE might reach extremely high viscosity values (~10 GPas)[36,43,44] which makes it difficult to process in its molten state. However, PTFE does not completely melt during ternary blends processing, but it reaches a gel-like state that increases blends viscosity with no evidence of negative effects on blends processability, since the less viscous phase, PBT, decreases the final torque in a similar way for binary and ternary blends by values close to 50%. These results suggest that both, binary and ternary blends, could be scale to industrial processing techniques such as extrusion or injection molding.

3.2 | Blends morphology

Figure 2 presents a general overview of the morphological evolution of ternary PEI/PBT/PTFE blends modified with 5, 10, and 15 wt% PTFE, as well as the comparison with the respective binary blends, named as 0 wt% PTFE in the figure. SEM micrographs of ternary blends show that increasing PEI concentration leads to similar

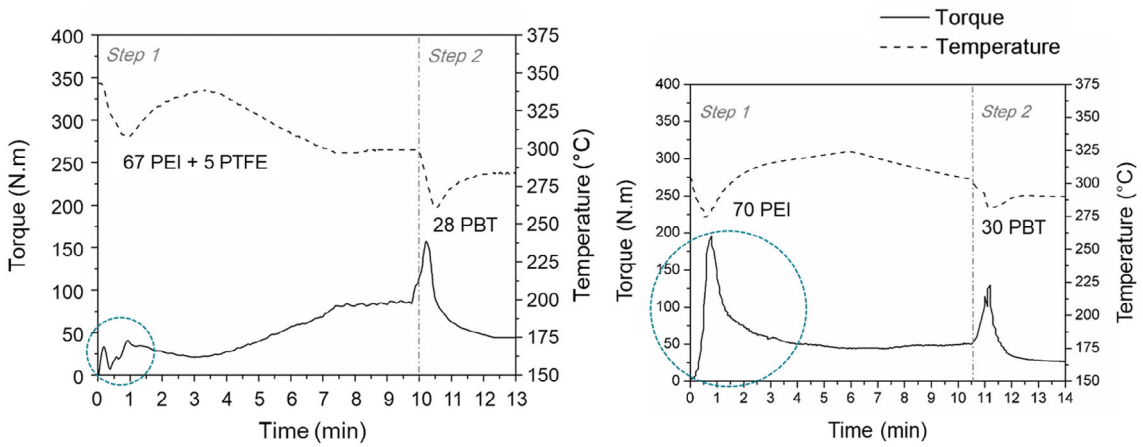

FIGURE 1 Torque and temperature as a function of time for 67/28/5 (left) and a binary 70/30 blend (right)

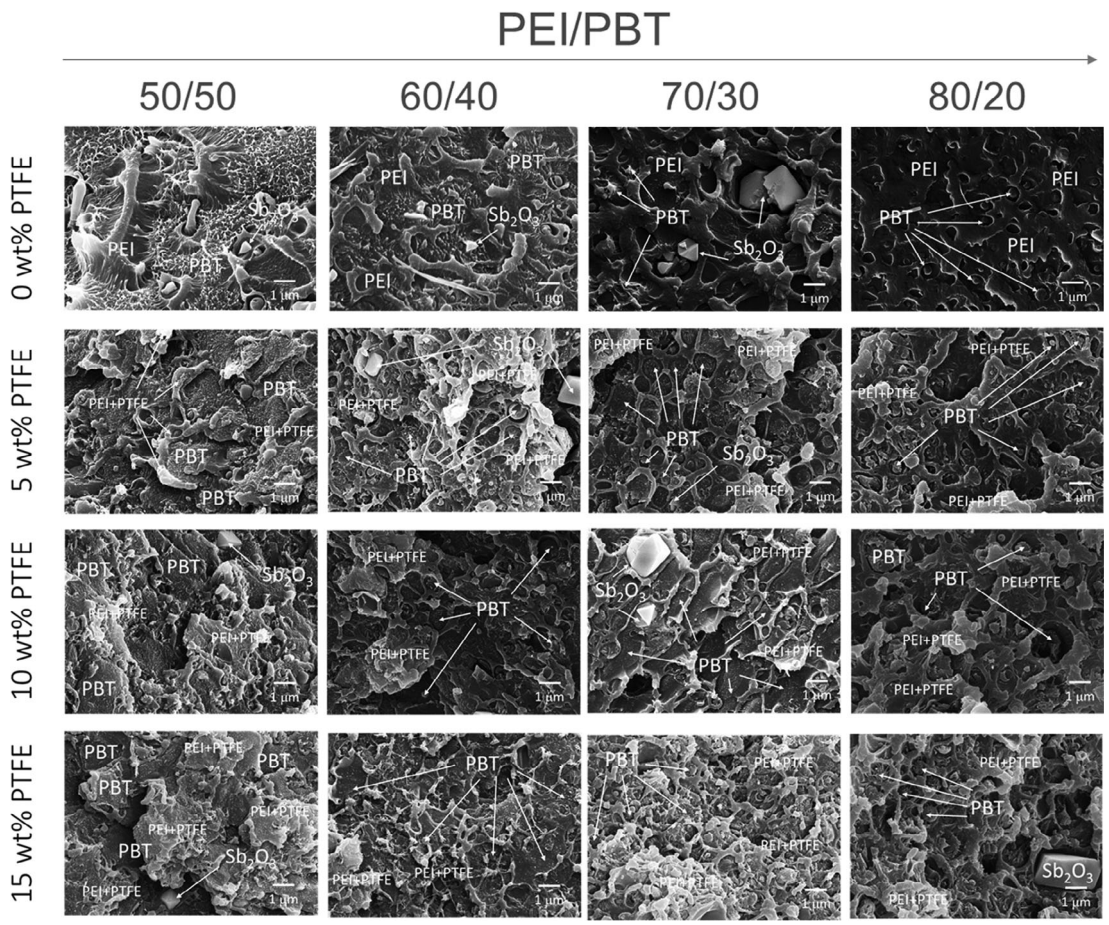

FIGURE 2 Morphology evolution of PEI/PBT blends modified with 5, 10, and 15 wt% PTFE

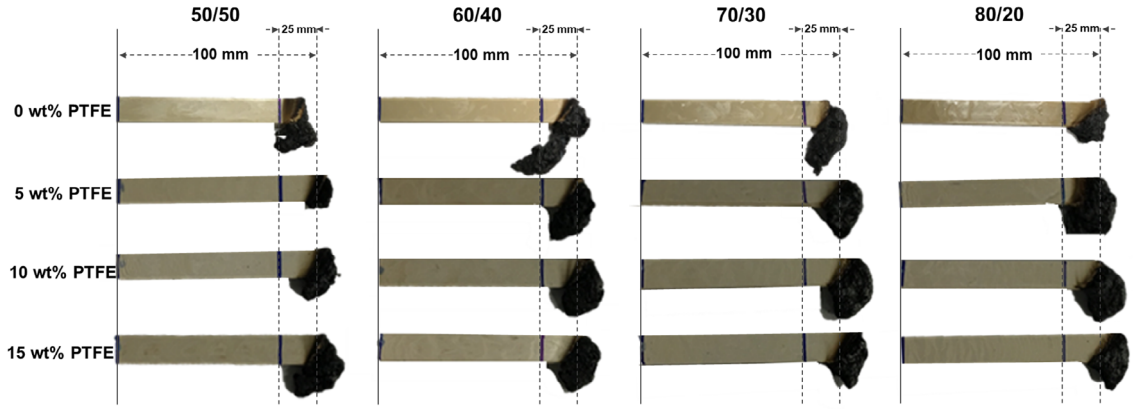

FIGURE 3 Photographs of binary and ternary blends specimens after the horizontal burning test. The composition of PEI/PBT blends is typed at the top of each block of four samples

morphological variations as those observed for binary ones,[30,40] and that PTFE does not interfere in PEI and PBT interfacial interaction. At 50 wt% PEI, a phase inversion phenomenon is revealed, and a co-continuous morphology is formed. The morphology evolves to PBT droplets embedded in the PEI matrix, which size reduces when PEI phase increases by the combined effect of shearing rate in the mixing chamber and high PEI viscosity.[40]

3.3 | Fire and combustion behavior

Figure 3 presents the HB test results for binary PEI/PBT and ternary PEI/PBT/PTFE blends after 4 minutes of direct flame exposure. The dashed lines delimit the maximum length of specimens before burning, as well as the first mark at 25 mm from the specimen's tip, which allows visualizing the spread of the flame along with the samples

according to UL94 standard.[45] As it is observed, flame did not overpass the first mark in any case, and the flame traces show lower flame propagation in ternary blends compare to that for binary blends. Hence, all ternary blends are classified as slow-burning specimens (HB), which is the maximum degree of flame-retardant for polymers that have a burning rate lower than 75 mm/min in a distance of 75 mm. This classification applies to samples of 3 mm thickness.

These results are expected since PTFE is an inherent flame-retardant polymer due to the fluorine atoms attached to its backbone chain, and the flame resistance is expected to be equal to or greater than that of binary PEI/PBT blends. Nevertheless, despite all blends exhibit intumescent layer formation, it calls attention that those for ternary blends exceed the upper dashed line limit, and seem larger than those for binary blends, which suggests that PTFE addition enhances the formation of the charring products. This is an unexpected result since PTFE does not exhibit charring products formation during thermal degradation, as presented in Figure S1b.

To better evaluate the effect of PTFE on blends flammability, the heat released during combustion is measured by the higher heating value (HHV) test. The HHV depends on the materials structure and composition, and in the case of polymers, is related to the amount of carbon and hydrogen in their structure and the chemical bonds between them. Additionally, HHV is known to decrease when species that inhibit charring formation increase, that is, sulfides, fluorides, among others.[46,47] The HHV test results for pure polymers show that PEI exhibits the highest value (32842.5 kJ/kg), while PBT shows a close value that is only 1.4 times lower (24025.0 kJ/kg). On the other hand, the HHV value for PTFE (6008.3 kJ/kg) is considerably lower than that of PEI (5.5 times lower), which is expected due to the fluorine present in its composition.

In Figure 4, it is shown the HHV analysis for ternary blends with 70 wt% PEI and 30 wt% PBT containing 5, 10, and 15 wt%. This PEI/PBT composition is chosen since it seems to produce the largest charring layer of all ternary blends. The experimental HHV results (continuous line) are compared with the theoretical values (dashed line) calculated from the additivity rule of blends.[17-20,48,49] It is noticed that increasing PTFE concentrations lead to a monotonical decrease in the heat released. This is to be expected since PTFE clearly exhibits the lowest value of all three polymers used in this work.

The heat released for the blend with 5 wt% PTFE is similar for both, measured and theoretical values. However, when PTFE amount increases, it is observed a negative deviation of experimental values from the additivity rule. Since this difference is accentuated by increasing the amount of fluorine in blends, it suggests this element contribute to these results. It is known that during blends combustion, the interaction between the components and their degradations products may cause deviations from additivity. Some authors report that in pyrolysis processes of materials containing halogenated compounds, the heat capacity decreases caused by a flame cooling effect. In the case of compounds with small amounts of PTFE, the accumulation of fluorine in the combustion residues could interact with other species, such as antimony groups, to give volatile moieties.[50]

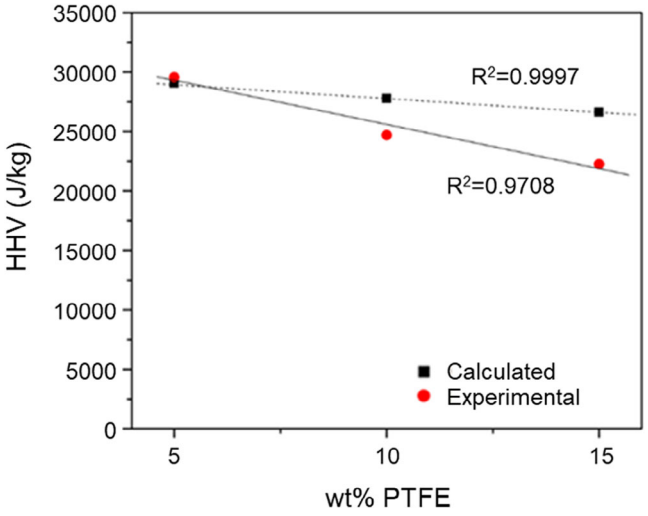

FIGURE 4 Calculated and experimental higher heating values (HHV) values of ternary PEI/PBT/PTFE blends containing 70 wt% PEI

3.4 | Thermal degradation analysis

TGA is used to better evaluate the interaction between blends components and their degradation products in the temperature range studied. On one hand, it is possible to understand the effect of PTFE on the thermal stability of blends and, on the other, on the production of carbonaceous residues.

In Figure 5, the results for pure PEI, PBT, PTFE, and ternary blends containing 5 wt% PTFE are presented. Only one concentration of PTFE is presented for demonstrative purposes since all ternary blends displayed the same behavior. Figure 5A shows that thermal decomposition of pure materials takes place in a single step and that at the difference of PEI and PBT, PFTE does not show any residue after 600°C, meaning that its flame protection process is not through intumescent layer formation. Figure 5B on the other hand, shows that each phase behavior is retained in the ternary blends, leading them to an intermediate three-step decomposition behavior.

The characteristic decomposition temperatures for binary and ternary blends are compared. Figure 6 shows the initial temperature (T_i), temperature at 10% of weight loss (T_{10}), and temperature at 40% of weight loss (T_{40}) for pure components, as well as for binary and ternary blends. Usually, the characteristic temperature analysis is performed at 50% weight loss (T_{50}).[51] However, since the total weight loss of PEI is lower than 50%, 40% is used for comparison purposes.

In our previous work,[40] it was found that PEI improves the thermal stability of PBT in binary PEI/PBT blends, and this behavior is still noticed in the characteristic temperatures of ternary blends by PTFE addition. In Figure 6A,B, it is shown an increase for T_i and T_{10} temperatures, respectively, due to increasing PTFE concentration from 5 to 15 wt%. Yet, has a thermal stability improvement is more noticeable in changes for T_{40} presented in Figure 6C, where the addition of PTFE to binary 50/50 blend, improves their thermal stability by 14%, 22%, and 24% from 5, 10, and 15 wt% of PTFE, respectively.

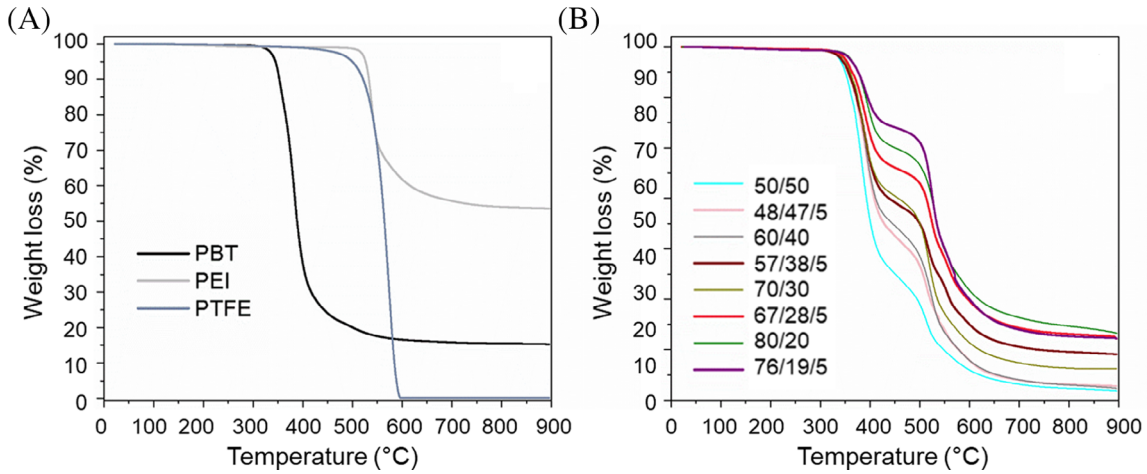

FIGURE 5 Thermal degradation analyses of: A, PEI, PBT, and PTFE and B, ternary PEI/PBT/PTFE blends with 5 wt% PTFE

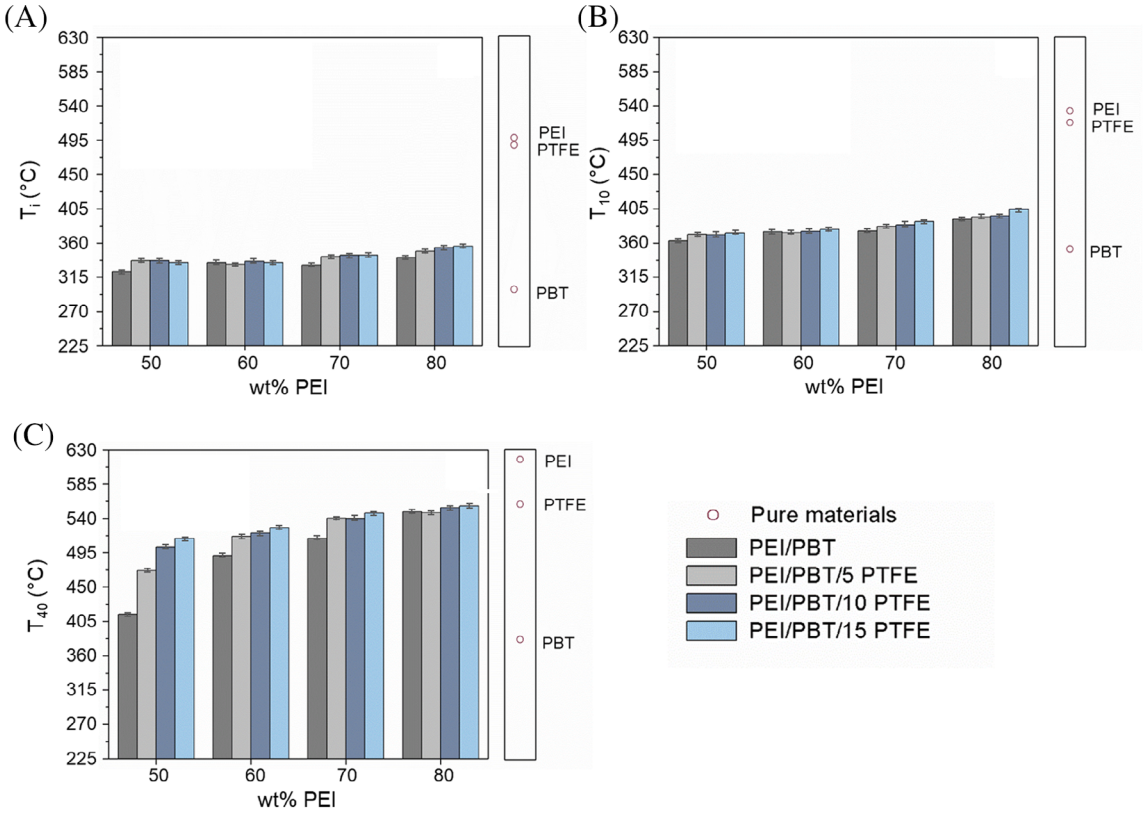

FIGURE 6 PTFE effect on the thermal stability of ternary PEI/PBT/PTFE blends: A, T_i, B, T_{10}, and C, T_{40}

It calls the attention that even though T_{40} temperature is increased by adding PTFE to binary blends containing 60, 70, and 80 wt% PEI, the improvement is not as noticeable as for 50 wt% PEI. This is explained from dual-phase morphology formed at this PEI concentration, and suggest that phase distribution strongly influences blends thermal performance. Furthermore, processing conditions enhance this particular behavior, since PTFE phase is added during step 1 in the blending process and it is preferably located in PEI phase, having a strong effect on the thermal stability of co-continuous ternary blends than in blends with droplet-like morphology.

Figure 7 presents the effect of PTFE on charring production as a function of PEI concentration, studied from comparing the char yield in TGA analysis. As expected, a gradual increase in carbonaceous residues is noticed at greater PEI concentrations. When comparing each group of blends, it is noticed that samples with the highest and the lowest PEI concentrations exhibited similar behavior. For these

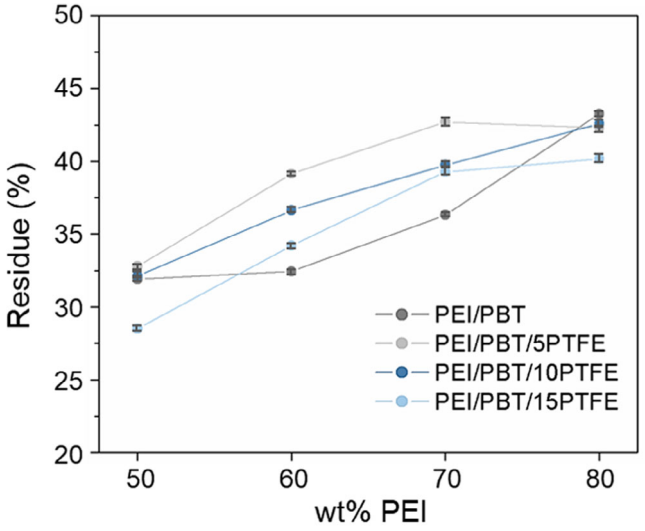

FIGURE 7 Experimental charring percentage of ternary PEI/PBT/PTFE blends as a function of PEI concentration

compositions, charring formation is independent of PTFE concentration as it is expected since blends containing higher PTFE concentrations (15 wt% PTFE) should generate lower charring products due to PTFE phase has no residues after TGA test.

However, the results observed in samples with intermediate amounts of PEI, 60 and 70 wt%, are quite different. Surprisingly, the addition of small amounts of PTFE increases their charring production, which systemically falls while PTFE concentration increases. These results confirm that low PTFE concentrations enhance intumescent layer formation, as observed in Figure 3, possibly caused by the interaction between the degradation products of PEI, PBT, and PTFE, which react in a fashion that improves the charring ability of ternary PEI/PBT/PTFE blends.

To confirm the above statement, theoretical TGA curves are calculated using the additivity rule. The resulting data represent the expected thermal behavior for each blend in the absence of interaction between polymers or their degradation product.[17-20,52] Figure 8 shows the comparison of experimental (solid lines) and calculated (dashed lines) TGA curves for ternary blends containing 5 wt% PTFE, as well as those of neat polymers.

Experimental and calculated curves exhibit three-step decomposition behavior corresponding to each polymer degradation. During the first step (PBT degradation), no difference is noticed between experimental and predicted curves, which confirms that PEI delays the initial degradation of PBT phase improving its thermal stability, as stated previously. However, clear differences between experimental and calculated curves start to appear just before the decomposition signal of the second step (PEI decomposition). The weight loss behavior of the experimental curves is lower than that of the theoretical curves. Additionally, the magnification presented in Figure 8B reveals the effect of adding 5 wt% PTFE on the generation of carbonaceous residues. Theoretical and experimental curves for blends with 50 and 80 wt% PTFE show no differences in the final residue, which is in good agreement with the results presented in Figure 7. However, blends with 60 and 70 wt% PEI, reveal that experimental carbonaceous residues (39.5% for 57/38/5 blend and 42.9% for 67/28/5 blend) are higher than the theoretical ones (36.6% for 57/38/5 and 40.1% for 67/28/5 blend). These results suggest that there is a synergistic contribution of PTFE to the flame resistance of ternary blends by intumescent layer production.

3.5 | XPS analysis of ternary blends

XPS results provide further information about the surface composition and content of ternary PEI/PBT/PTFE blends, as well as the interaction between blend components and their degradation products.

The XPS survey spectra of ternary PEI/PBT/PTFE blends with 70 wt% PEI before and after burning tests (Figure S2), reveals that these two types of samples contain identical elements of F, C, O, Sb, C, and Br. Nevertheless, their narrow XPS spectra exhibit marked differences. Figure 9 shows XPS narrow C 1s spectra of 63/27/10 ternary blends before and after HB tests. In the sample before calcination (Figure 9A), the C1s photoelectron peak decomposes into five components. These can be assignable to C—C (284.8 eV), attributed to aromatic and aliphatic carbons, C—O (285.8 eV) in carbonyl groups of PEI and PBT, NC═O (288.1 eV), assigned to the succinimide groups of PEI,[53] COO (289.2 eV) in the carboxylic group of PBT,[54] and CF_2 (292.2 eV) of PTFE.[55] However, after HB test (Figure 9B), two more components related to C—F bond are found. These new peaks appear at 290.4 and 293.2 eV, and are assigned to CF and CF_3 groups, respectively.[56] The alteration of the chemical structure of CF_2 group is probably due to the action of chemically reactive PTFE degradation products, such as COF_X species produced in the oxidation of ternary PEI/PBT/PTFE during the burning process.[56,57] Studies about PTFE pyrolysis suggested a selective cracking of C_2F_4 units and the formation of CF and CF_3 species by secondary reactions during combustion.[58] That selective cracking of C_2F_4 units has low energy requirements, as shown by the HHV results in Figure 4.

Additional information is revealed when the F 1s signal is studied. Figure 10 shows the narrow spectra of F 1s energy region for PEI/PBT (70/30) blend with different wt% PTFE after HB tests. Peak fitting of this signal shows the presence of CF_x species at 688.7 (F_I), 689.9 (F_{II}), and 691.4 (F_{III}) eV. The F_{II} peak is attributed to CF_2 group, which constitutes the PTFE structure, as previously observed in C 1 s region.[58] However, the interpretation of F_I and F_{III} peaks in the literature is ambiguous, and *a deeper analysis is required*.[53] To clarify this, we calculated the difference between the binding energy (ΔBE) positions of F_I and F_{III} peaks with respect to the F_{II} position in the PTFE structure (689.9 eV). F_I and F_{II} peaks are separated by about 1.2 eV. According to the literature, this value has two possible interpretations for F_I peak: (a) attributed to semi-ionic CF bonds[59] and (b) attributed to the presence of fluorinated polymers with an atomic fluorine/carbon (F/C) ratio of 1.2.[60] On the other hand, F_{II} and F_{III} peaks are separated by about 1.5 eV. Zhang et al[61] reported that this difference corresponds to COF_x bonds.

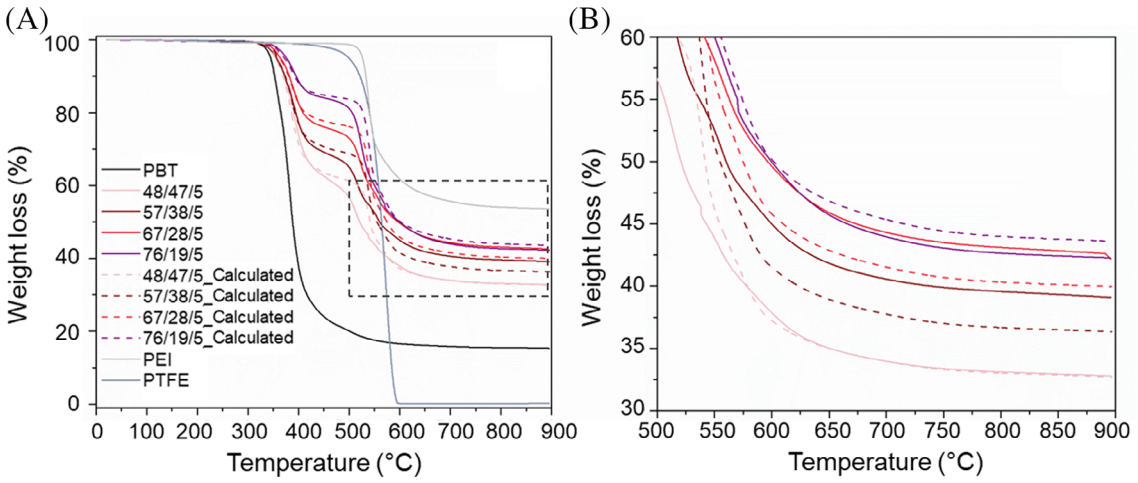

FIGURE 8 Thermogravimetric analysis (TGA) for ternary PEI/PBT/PTFE blends containing 5 wt% PTFE: A, Experimental and calculated curves, and B, Zoom in of experimental and calculated carbonaceous products

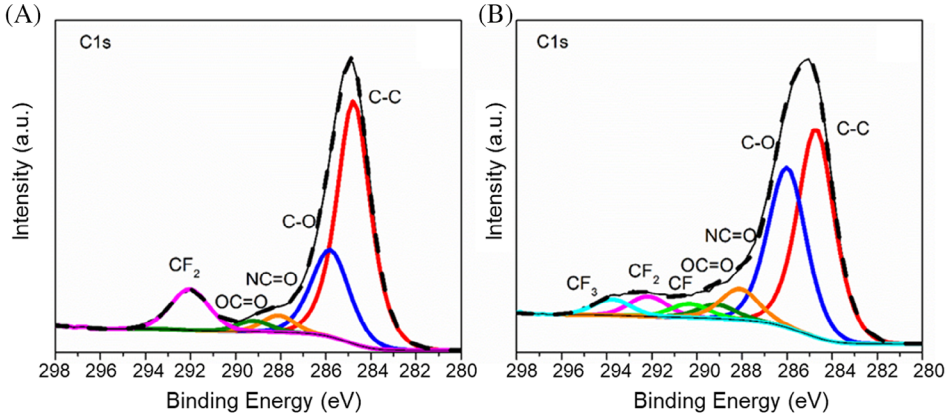

FIGURE 9 Typical C 1s XPS spectra of ternary 63/27/10 blend and its peak fitting, A, before and B, after the horizontal burning test

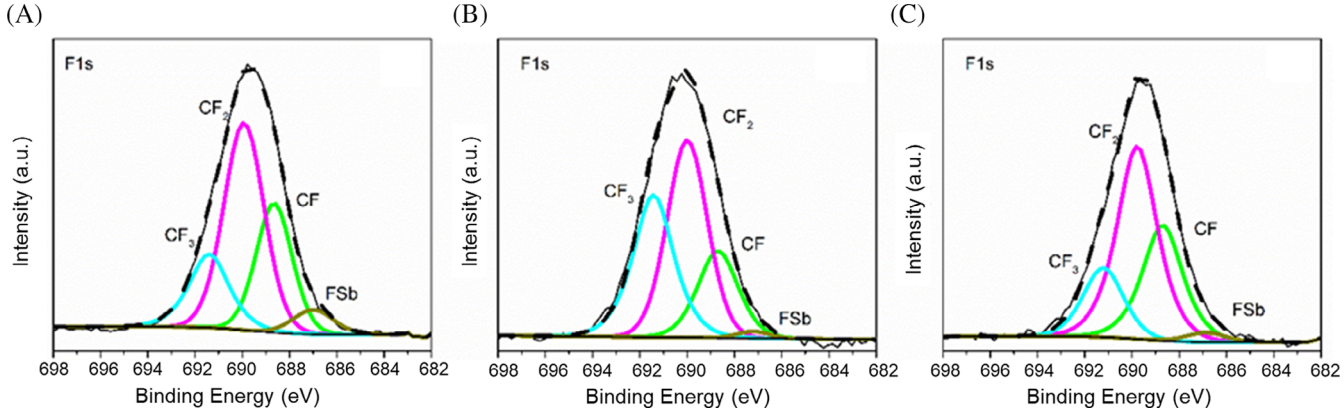

FIGURE 10 F 1s narrow XPS spectrum of ternary PEI/PBT/PTFE blends containing 70 wt% of PEI for: A, 5 wt% PTFE, B, 10 wt% PTFE, and C, 15 wt% PTFE after horizontal burning tests

In addition, in F 1s binding region in Figure 10 it is possible to identify the presence of antimony groups at 687.0 eV, attributed to the Sb-F species.[54] Some studies, which evaluated the addition of small amounts PTFE to other polymers with the aim of avoiding the dripping effect, suggested that the chemical interaction between PTFE and Sb led to SbF_3 formation.[51,62] They also pointed out that this species acts as a catalyst, increasing the formation of charring products. According to this, Sb-F species observed in this work could be a result of the chemical interaction between PTFE and Sb_2O_3, present in PBT. It is important to note that this effect is caused by the

calcination process, since no peaks of Sb-F species were observed in 70/30 PEI/PBT/PTFE samples before HB test (Figure S3). These results suggest that Sb-F species production during calcination could be the cause of the increase in charring formation.

Although the areas of F-Sb signals at the surface are small in relation to the entire F peak, they have been determined. The F atom percentages of F-Sb bond is ~6% for the sample with 5 wt% PTFE, and decreases to ~1% and ~ 2% for blends with 10 and 15 wt% PTFE, respectively. If these results are compared with the amount of charring production in PEI/PBT (70/30) samples after the TGA test (Figure 7), it is observed that they follow the same trend. Thus, 67/28/5 blend is the one that suffered the greatest charring production, and also the one with the highest Sb-F species presence (~6%). Similarly, the charring production in 63/27/10 and 60/25/15 blends is very similar and lower than observed for 67/28/5, as well as the presence of Sb-F species, which in these cases were ~ 1% and ~ 2%, respectively. This data supports the idea that Sb-F species produced during the combustion would be responsible for the increase in charring product formation.

The presence of Sb-F species is further confirmed by Sb 3d and Sb 4d spectra analysis (Figures S4 and S5). In 3d region, SbF_3 is confirmed at 531.7 ($3d_{5/2}$) and 541.0 eV ($3d_{3/2}$), while in 4d region the peaks at 35.8 ($3d_{5/2}$) and 37.0 eV ($3d_{3/2}$) are assigned to Sb-F species.[63]

4 | CONCLUSIONS

Ternary PEI/PBT/PTFE blends were produced using a two-step processing method for PEI concentrations higher than 50 wt%, and different concentrations of PTFE. PTFE incorporation did not affect blends processability or interaction between PEI and PBT phases, and the same morphologies as those of binary PEI/PBT blends were obtained.

It was noticed that PTFE addition inhibits flame propagation of binary PEI/PBT blends, and all samples are classified as slow-burning materials according to UL94 standard. Additionally, the HHV tests revealed that the presence of PTFE reduces the heating energy and promotes a flame cooling effect. Regarding TGA results, it was noticed that PTFE improves the thermal stability of all blends, in particular for that with 50 wt% PEI, where a co-continuous morphology is promoted.

It was noticed that the major flame protection process for all blends is the charring production, and that small amounts of PTFE improved the charring production of blends containing 60 wt% PTFE and 70 wt% PTFE. Even, a synergic effect is observed when experimental and theoretical charring production values from TGA results are compared, suggesting that there is an interaction effect between PTFE and PEI and PBT and their degradation products. These results were contrasted with XPS analyses. Detailed spectra on C 1s and F 1s energy regions indicated the appearance of new C-F species after the HB test due to the oxidation during the burning process. In addition, F 1s, Sb 3d, and Sb 4d peaks indicated the appearance of SbF species, which confirmed the interaction between blend components and their degradation products. It is also highlighted the important role of SbF species in the charring product formation during the ternary PEI/PBT/PTFE blends burning process.

ACKNOWLEDGEMENTS

The authors would like to acknowledge the financial support from Instituto Tecnológico Metropolitano, Universidad EAFIT, project Fondecyt 11190841, the program VID in the framework of "U-Inicia" UI 003/2018 and Laboratorio de Superficies y Materiales (FCFM, Universidad de Chile).

DATA AVAILABILITY STATEMENT

The raw data and processed data required to reproduce these findings are available to download from http://dx.doi.org/10.17632/yn4yxgbxxw.1.

ORCID

Mauricio Vásquez-Rendón https://orcid.org/0000-0002-9078-3111
Mónica L. Álvarez-Láinez https://orcid.org/0000-0002-4031-9089

REFERENCES

1. Bajaj P. Fire-retardant materials. *Bull Mater Sci*. 1992;15:67-76.
2. Horrocks AR. Developments in flame retardants for heat and fire resistant textiles—the role of char formation and intumescence. *Polym Degrad Stab*. 1996;54:143-154.
3. Bajaj P, Agrawal AK, Dhand A, Kasturia N, Hansraj. Flame retardation of acrylic fibers: an overview. *J Macromol Sci Part C Polym Rev*. 2000;40:309-337.
4. Tsai P. Performance of masks and discussion of the inactivation of SARS-CoV-2. *Eng Sci*. 2020;10:1-7. https://doi.org/10.30919/es8d1110.
5. Liu K, Liu Y, Lin D, Pei A, Cui Y. Materials for lithium-ion battery safety. *Sci Adv*. 2018;12:1-11.
6. Liu Y, Zhang H, Porwal H, Busfield JJ, Peijs T, Bilotti E. Pyroresistivity in conductive polymer composites: a perspective on recent advances and new applications: pyroresistivity in conductive polymer composites. *Polym Int*. 2019;68:299-305. https://doi.org/10.1002/pi.5735.
7. Patil A, Patel A, Purohit R. An overview of polymeric materials for automotive applications. *Mater Today Proc*. 2017;4:3807-3815. https://doi.org/10.1016/j.matpr.2017.02.278.
8. Bar M, Alagirusamy R, Das A. Flame retardant polymer composites. *Fibers Polym*. 2015;16:705-717. https://doi.org/10.1007/s12221-015-0705-6.
9. Zhang D, Williams BL, Santos VH, et al. Self-assembled intumescent flame retardant coatings: influence of pH on the flammability of cotton fabrics. *Eng Sci*. 2020;12:106-112. https://doi.org/10.30919/es8d1134.
10. Das R, Vupputuri S, Hu Q, et al. Synthesis and characterization of antiflammable vinyl ester resin nanocomposites with surface functionalized nanotitania. *ES Mater Manuf*. 2020;8:46-53. https://doi.org/10.30919/esmm5f709.
11. Lu C, Gao X, Yao D, Cao C, Luo Y. Improving flame retardancy of linear low-density polyethylene/nylon 6 blends via controlling localization of clay and intumescent flame-retardant. *Polym Degrad Stab*. 2018;153:75-87. https://doi.org/10.1016/j.polymdegradstab.2018.04.022.
12. Sanchez-Olivares G, Sanchez-Solis A, Manero O, et al. Improving mechanical properties and reaction to fire of EVA/LLDPE blends for cable applications with melamine triazine and bentonite clay. *Materials*. 2019;12:2393. https://doi.org/10.3390/ma12152393.

13. Lu C, Gao X, Yang D, et al. Flame retardancy of polystyrene/nylon-6 blends with dispersion of clay at the interface. *Polym Degrad Stab*. 2014;107:10-20. https://doi.org/10.1016/j.polymdegradstab.2014.04.028.
14. Sonnier R, Taguet A, Ferry L, Lopez-Cuesta J-M. Flame retardant bio-based polymers. *Bio-based Flame Retardant Polymers*. Cham, Switzerland: Springer International Publishing; 2018:1-32. https://doi.org/10.1007/978-3-319-67083-6_1.
15. Hobbs C. Recent advances in bio-based flame retardant additives for synthetic polymeric materials. *Polymers*. 2019;11:224. https://doi.org/10.3390/polym11020224.
16. Köppl T, Brehme S, Pospiech D, et al. Influence of polymeric flame retardants based on phosphorus-containing polyesters on morphology and material characteristics of poly(butylene terephthalate). *J Appl Polym Sci*. 2013;128:3315-3324. https://doi.org/10.1002/app.38520.
17. Dodson B, McNeill IC. Degradation of polymer mixtures. VI. Blends of poly (vinyl chloride) with polystyrene. *J Polym Sci Polym Chem Ed*. 1976;14:353-364.
18. Naffakh M, Ellis G, Gómez MA, Marco C. Thermal decomposition of technological polymer blends 1. Poly(aryl ether ether ketone) with a thermotropic liquid crystalline polymer. *Polym Degrad Stab*. 1999;66:405-413.
19. McNeill IC, Gorman JG, Basan S. Thermal degradation of blends of PVC with poly (tetramethylene sebacate). *Polym Degrad Stab*. 1991;33:263-276.
20. Campoy I, Gómez MA, Marco C. Thermogravimetric analysis of blends based on nylon 6 and a thermotropic liquid crystal copolyester. *J Thermal Anal*. 1998;52:705-715.
21. Vahabi H, Dumazert L, Khalili R, Saeb MR, Cuesta J-ML. Flame retardant PP/PA6 blends: a recipe for recycled wastes. *Flame Retard Therm Stab Mater*. 2019;2:1-8. https://doi.org/10.1515/flret-2019-0001.
22. Viretto A, Taguet A, Sonnier R. Selective dispersion of nanoplatelets of MDH in a HDPE/PBT binary blend: effect on flame retardancy. *Polym Degrad Stab*. 2016;126:107-116. https://doi.org/10.1016/j.polymdegradstab.2016.01.021.
23. Zou W, Huang J, Zeng W, Lu X. Effect of ethylene-butylacrylate-glycidyl methacrylate on compatibility properties of poly (butylene terephthalate)/ thermoplastic polyurethane blends. *ES Energy Environ*. 2020;9:67-73. https://doi.org/10.30919/esee8c180.
24. Utracki LA. *Polymer Blends Handbook*. Dordrecht, the Netherlands: Kluwer; 2002.
25. Horrocks AR. Technical fibers for heat and flame protection. *Handbook of Technical Textiles: Technical Textile Applications*. Second ed. England: Woodhead Publishing, Woodhead Publishing Series in Textiles; 2016.
26. Horrocks AR. Flame retardant challenges for textiles and fibres: new chemistry versus innovatory solutions. *Polym Degrad Stab*. 2011;96:377-392. https://doi.org/10.1016/j.polymdegradstab.2010.03.036.
27. Horrocks AR, Kandola BK, Davies PJ, Zhang S, Padbury SA. Developments in flame retardant textiles - a review. *Polym Degrad Stab*. 2005;88:3-12. https://doi.org/10.1016/j.polymdegradstab.2003.10.024.
28. Sato H, Kondo K, Tsuge S, Ohtani H, Sato N. Mechanisms of thermal degradation of a polyester flame-retarded with antimony oxide/brominated polycarbonate studied by temperature-programmed analytical pyrolysis. *Polym Degrad Stab*. 1998;62:41-48.
29. Montezin F, Lopez-Cuesta J-M, Crespy A, Georlette P. Flame retardant and mechanical properties of a compolymer PP/PE containing brominated compounds/antimony trioxid blends and magnesium hydrixide or talc. *Fire Mater*. 1997;21:245-252.
30. Vásquez-Rendón M, Sánchez-Arrieta N, Álvarez-Láinez M. Two-step processing method for blending high-performance polymers with notable thermal and rheological differences: PEI and PBT. *Polym Plast Technol Eng*. 2017;57:1411-1417. https://doi.org/10.1080/03602559.2017.1381256.
31. Ren J. Tribological properties of Xytrex® polymers of 3P corporation. *Global Advances in Materials and Process Engineering: SAMPE Fall Technical Conference*. 38. Dallas, TX: Society for the Advancement of Material and Process Engineering; 2006.
32. Mu L, Zhu J, Fan J, et al. Self-lubricating polytetrafluoroethylene/polyimide blends reinforced with zinc oxide nanoparticles. *J Nanomater*. 2015;2015:1-8. https://doi.org/10.1155/2015/545307.
33. Chen B, Wang J, Yan F. Microstructure of PTFE-based polymer blends and their tribological behaviors under aqueous environment. *Tribol Lett*. 2012;45:387-395. https://doi.org/10.1007/s11249-011-9896-1.
34. Bijwe J, Sen S, Ghosh A. Influence of PTFE content in PEEK-PTFE blends on mechanical properties and tribo-performance in various wear modes. *Wear*. 2005;258:1536-1542. https://doi.org/10.1016/j.wear.2004.10.008.
35. Bijwe J, Tewari US, Vasudevan P. Friction and wear studies of an internally lubricated polyetherimide composite. *J Synth Lubr*. 1989;6:179-202.
36. Zhang J, Demas NG, Polycarpou AA, Economy J. A new family of low wear, low coefficient of friction polymer blend based on polytetrafluoroethylene and an aromatic thermosetting polyester. *Polym Adv Technol*. 2008;19:1105-1112. https://doi.org/10.1002/pat.1086.
37. Hussain M, Ko YH, Choa YH. Significant enhancement of mechanical and thermal properties of thermoplastic polyester elastomer by polymer blending and nanoinclusion. *J Nanomater*. 2016;2016:1-9. https://doi.org/10.1155/2016/8515103.
38. Anbinder PS, Peruzzo PJ, de Siervo A, Amalvy JI. Surface, thermal, and mechanical properties of composites and nanocomposites of polyurethane/PTFE nanoparticles. *J Nanopart Res*. 2014;16:1-11. https://doi.org/10.1007/s11051-014-2529-5.
39. Palabiyik M, Bahadur S. Tribological studies of polyamide 6 and high-density polyethylene blends filled with PTFE and copper oxide and reinforced with short glass fibers. *Wear*. 2002;253:369-376.
40. Vásquez-Rendón M, Álvarez-Láinez ML. Tailoring the mechanical, thermal, and flammability properties of high-performance PEI/PBT blends exhibiting dual-phase continuity. *Polymer*. 2018;154:241-252. https://doi.org/10.1016/j.polymer.2018.09.012.
41. Khedkar J, Negulescu I, Meletis EI. Sliding wear behavior of PTFE composites. *Wear*. 2002;252:361-369. https://doi.org/10.1016/S0043-1648(01)00859-6.
42. Conte M, Igartua A. Study of PTFE composites tribological behavior. *Wear*. 2012;296:568-574. https://doi.org/10.1016/j.wear.2012.08.015.
43. Blumm J, Lindemann A, Meyer M, Strasser C. Characterization of PTFE using advanced thermal analysis techniques. *Int J Thermophys*. 2010;31:1919-1927. https://doi.org/10.1007/s10765-008-0512-z.
44. Case LC. Viscosity of polytetrafluoroethylene above the melting point. *J Appl Polym Sci*. 1960;3:254-254.
45. American National Standards Institute. *Underwriters' Laboratories, Standard for tests for flammability of plastic materials for parts in devices and appliances*. Northbrook, IL: Underwriters' Laboratories; 2001.
46. Walters RN, Hackett SM, Lyon RE. Heats of combustion of high temperature polymers. *Fire Mater*. 2000;24:245-252.
47. Gong J, Chen X, Tang T. Recent progress in controlled carbonization of (waste) polymers. *Prog Polym Sci*. 2019;94:1-32. https://doi.org/10.1016/j.progpolymsci.2019.04.001.
48. Amin A, Gadallah A, El Morsi AK, El-Ibiari NN, El-Diwani GI. Experimental and empirical study of diesel and castor biodiesel blending effect, on kinematic viscosity, density and calorific value. *Egypt J Pet*. 2016;25:509-514. https://doi.org/10.1016/j.ejpe.2015.11.002.
49. Sajdak M. Impact of plastic blends on the product yield from co-pyrolysis of lignin-rich materials. *J Anal Appl Pyrolysis*. 2017;124:415-425. https://doi.org/10.1016/j.jaap.2017.03.002.
50. Roma P, Camino G, Luda MP. Mechanistic studies on fire retardant action of fluorinated additives in ABS. *Fire Mater*. 1997;21:6.

51. Zhao H, Chen L, Yun J, et al. Improved thermal stabilities, ablation and mechanical properties for carbon fibers/phenolic resins laminated composites modified by silicon-containing polyborazine. *Eng Sci*. 2018;2:57-66. https://doi.org/10.30919/es8d726.
52. Ray I, Roy S, Khastgir D. Interaction between ethylene vinyl acetate copolymer and polyethylene. *Polym Bull*. 1993;30:685-689.
53. Burrell MC, Chera JJ. Polyetherimide (Ultem ®) spin cast films by XPS. *Surf Sci Spectra*. 1999;6:18-22. https://doi.org/10.1116/1.1247898.
54. Burrell MC, Chera JJ. Polybutylene terephthalate (PBT) spin cast films by XPS. *Surf Sci Spectra*. 1999;6:5-8. https://doi.org/10.1116/1.1247895.
55. Girardeaux C, Pireaux J-J. Analysis of poly(tetrafluoroethylene) (PTFE) by XPS. *Surf Sci Spectra*. 1996;4:138-141. https://doi.org/10.1116/1.1247814.
56. Vesel A, Mozetic M, Zalar A. XPS characterization of PTFE after treatment with RF oxygen and nitrogen plasma. *Surf Interface Anal*. 2008;40:661-663. https://doi.org/10.1002/sia.2691.
57. Xu J, Zhang Q, Cheng Y-T. High capacity silicon electrodes with nafion as binders for lithium-ion batteries. *J Electrochem Soc*. 2016;163:A401-A405. https://doi.org/10.1149/2.0261603jes.
58. Tolstopyatov EM. Ablation of polytetrafluoroethylene using a continuous CO_2 laser beam. *J Phys Appl Phys*. 2005;38:1993-1999. https://doi.org/10.1088/0022-3727/38/12/021.
59. Simon CM, Kaminsky W. Chemical recycling of polytetrafluoroethylene by pyrolysis. *Polym Degrad Stab*. 1998;62:1-7. https://doi.org/10.1016/S0141-3910(97)00097-9.
60. Ferraria AM, Lopes da Silva JD, Botelho do Rego AM. XPS studies of directly fluorinated HDPE: problems and solutions. *Polymer*. 2003;44:7241-7249. https://doi.org/10.1016/j.polymer.2003.08.038.
61. Zhang F-Y, Advani SG, Prasad AK, Boggs ME, Sullivan SP, Beebe TP. Quantitative characterization of catalyst layer degradation in PEM fuel cells by X-ray photoelectron spectroscopy. *Electrochim Acta*. 2009;54:4025-4030. https://doi.org/10.1016/j.electacta.2009.02.028.
62. Feng W, Long P, Feng Y, Li Y. Two-dimensional fluorinated graphene: synthesis, structures, properties and applications. *Adv Sci*. 2016;3:1500413. https://doi.org/10.1002/advs.201500413.
63. Moura CA d S, Belmonte GK, Reddy PG, Gonslaves KE, Weibel DE. EUV photofragmentation study of hybrid nonchemically amplified resists containing antimony as an absorption enhancer. *RSC Adv*. 2018;8:10930-10938. https://doi.org/10.1039/C7RA12934C.

SUPPORTING INFORMATION

Additional supporting information may be found online in the Supporting Information section at the end of this article.

How to cite this article: Vásquez-Rendón M, Romero-Sáez M, Mena J, Fuenzalida V, Berlanga I, Álvarez-Láinez ML. Synergistic contribution on flame retardancy by charring production in high-performance PEI/PBT/PTFE ternary blends: The role of PTFE. *Polym Adv Technol*. 2021;32:1615–1625. https://doi.org/10.1002/pat.5198